J Wood Sci (2003) 49:145–151

ORIGINAL ARTICLE

Nicolas Richard · Motoi Yasumura · Luc Davenne

Prediction of seismic behavior of wood-framed shear walls with openings by pseudodynamic test and FE model

Received: February 15, 2002 / Accepted: April 25, 2002

Abstract This article summarizes an experimental and numerical study on seismic behavior of wood-framed shear walls with an opening. The objectives of this study were to compare the results of static and pseudodynamic tests of plywood-sheathed shear walls with numerical simulation by the Finite Element (FE) model and to validate a finite element code EFICOBOIS for such an application. This software is based on a macroelement approach to limit the number of degrees of freedom for the whole system. Nonlinear laws for connections such as nails and hold-down connections, among others, are applied through macroelements that link plate elements to beam elements. Numerical results obtained for the various loading conditions showed good agreement with the experiments. Both static and dynamic computations are presented here.

Key words Wood-framed shear walls · FE model · Pseudodynamic test

Introduction

Properly designed light-framed buildings consisting of wood-based shear walls have performed generally well during earthquakes. For example, in the 1995 Hyogo-ken Nanbu earthquake, such buildings survived high seismic forces with little damage. Some buildings with large openings and irregular plan layouts, however, did not perform adequately against severe earthquakes. This poor performance caused many fatalities and high financial losses, as experienced in the 1994 Northridge earthquake. Therefore, researchers have been prompted to examine the performance of wood-framed structures under extreme seismic loading.

It is expensive to test full-scale structures on a shake table, so it is essential to develop numerical tools including those that evaluate the nonlinear behavior of the connections used in the structure. A French-Japanese project was established to validate a model that predicts more accurately the seismic performance of wood-framed structures. Static and pseudodynamic tests were conducted on wood-framed shear walls with an opening at Shizuoka University, Japan. These experimental results were compared with numerical results obtained using a finite element code EFICOBOIS, developed at the Laboratoire de Mécanique et Technologie, E.N.S. Cachan, France.[1–4] The results of the static analysis were compared with those of monotonic and reversed cyclic loading; and then those of the dynamic analysis were compared with the pseudodynamic test results. The numerical results of both the static and dynamic analyses showed comparatively good agreement with the experimental results, and it was proved that the software reliably predicts the seismic behavior of wood-framed shear walls.

N. Richard · L. Davenne
Laboratoire de Mécanique et Technologie, E.N.S. Cachan 94235, France

M. Yasumura (✉)
Faculty of Agriculture, Shizuoka University, Shizuoka 422-8529, Japan
Tel. +81-54-238-4863; Fax +81-54-237-3028
e-mail: afmyasu@agr.shizuoka.ac.jp

Materials and methods

Specimens

Specimens had the same structure as presented in a previous study.[5] They had wooden frames of 2.73 m length and 2.44 m height with an opening 910 mm in width and 1000 mm in height at the center of the wall. The specimens were constructed according to Japanese building codes.[6] Spruce plywood 9.5 mm thick was sheathed on one side of the wall by a frame consisting of nominal two-by-four lumbers of S-P-F STANDARD. Sheathing materials were connected to the wooden frame with JIS A5508 CN50 nails (50.8 mm length, 2.87 mm diameter). Studs were spaced 455 mm apart and were connected to the bottom and double top plates

with CN90 nails (88.9 mm length, 4.11 mm diameter). Hold-down connections (HD20) were applied to connect the triple studs at both ends of the wall and both sides of the opening to the steel foundation with four lag-screws of 12 mm diameter. A lintel consisting of two two-by-six lumbers and a 9.5 mm thick plywood spacer was placed above the opening.

Test methods

The bottom plates of the wall panels were connected to an 89 × 89 mm sill and steel foundation with four bolts of 16 mm diameter. Double top plates were connected to an 89 × 89 mm girder with four bolts and hold-down connections (HD15) placed at both ends of the wall. The monotonic and reversed cyclic loads were applied at the end of the girder by an actuator with a capacity of ±150 kN and a stroke of ±200 mm controlled by a Shimadzu 48000 system. Horizontal and vertical displacements of the wall were measured with electronic transducers. One specimen was subjected to monotonic loading; then reversed cyclic loading based on the loading protocol shown in Fig. 1 was applied to another specimen.

Pseudo-dynamic tests were also conducted on shear walls of the same configuration. The earthquake accelerograms were based on the records of N-S components of the 1995 JMA Kobe and 1992 Landers earthquakes. They were linearly scaled to have a maximum acceleration of 0.4 g. The damping and mass were 2% and 7000 kg, respectively. The mass was determined based on an ultimate load of 23.7 kN for the monotonic loading test and a structural behavior factor (D_s) of 0.35 calculated by the following equation.

$$D_s = \frac{1}{\sqrt{2\mu - 1}}; \quad \mu = \frac{D_u}{D_y} \times \frac{P_y}{P_u} \tag{1}$$

where, D_y and D_u are the yield and ultimate displacements, and P_y and P_u are the yield and ultimate loads, respectively.

General description of model

Only an outline of the model is described herein because the main objective of this study was to validate the model. The model used in this study is described more precisely in the literature.[7]

The model consists of beam elements for wooden frames, plate elements for plywood sheathings, and joint elements connecting two frame members; studs to the foundation; and plywood sheathing to frame members, as shown in Fig. 2. In the simulation, all the non-linearity is supposed to take place in the connections. The framing is modeled with two nodes of elastic beam elements and the sheathing with four nodes of elastic orthotropic plate elements. A framing connection is modeled with a nonlinear spring system that relates the degrees of freedom (relative displacements and rotations) of the end nodes of the considered beam elements. Because there are many nail connections between a beam and a plate, they are considered using a global approach as shown in Fig. 3, without adding new degrees of freedom to the simulation. The relative displacement of the joint is computed using the shape functions of the plate element and the beam element. The stiffness of the connection is assembled in the global stiffness matrix without adding new equations. For the global motion equations, a Newmark algorithm is used. The material nonlinearity is solved with an initial strain algorithm. Keeping the initial stiffness, the convergence is made on nonelastic forces computed at each step. A classical Newton Raphson method is used for the convergence. The contact between two sheathing plates and the resulting intercrushing is not considered in the model. Nevertheless, during the tests on shear walls with an opening, a full row of nails connecting the sheathing to the studs on each side of the opening were rapidly pulled out after the peak load owing to the out-of-plane displacement induced by this contact.

Model for nailed connection

The proposed model for a connection consists of a nonlinear relation between the force F and the relative displace-

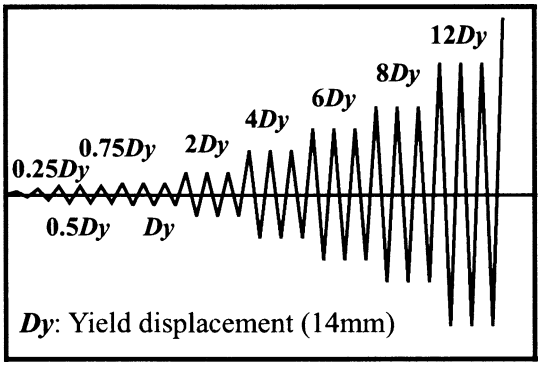

Fig. 1. Loading protocol for the reversed cyclic test

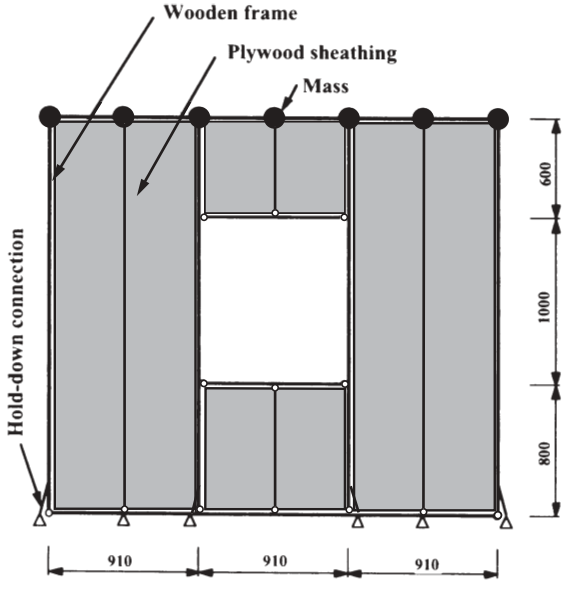

Fig. 2. Modeling of the shear wall

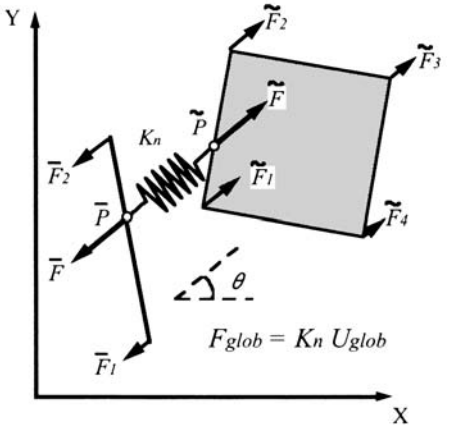

Fig. 3. Proposed joint element

ment Δ of the constitutive elements of the beam and plate. It is therefore a phenomenological approach. The hypothesis assumes that the relative drift direction varies little during the loading history. As a consequence, it was supposed that uniaxial tests on these connections are sufficient to determine the parameters of the model. The global nonlinear behavior of a nail-type connection is based on the crushing of the surrounding wood, the formation of a plastic hinge in the shank of the nail, friction between the nail and the wood, and sliding of the nail or crushing of the panel by the nail head (or both).

The following rules, as shown in Fig. 4, are proposed for modeling the uniaxial response. For monotonic loading, an exponential relation[8] followed by linear postpeak softening and completed with a second linear decrease and a cutting-off of the strength corresponding to the failure were adopted:

$$F(\Delta) = (P_0 + K_1\Delta)\times\left[1 - \exp(-K_0\Delta/P_0)\right] \quad \text{when } 0 \le \Delta \le D_1 \tag{2}$$

$$F(\Delta) = F_{\max} + K_2(\Delta - D_1) \quad \text{when } D_1 \le \Delta \le D_2 \tag{3}$$

$$F(\Delta) = F_{\max} + K_2(D_2 - D_1) + K_3(\Delta - D_2) \quad \text{when } D_2 \le \Delta \le D_{\max} \tag{4}$$

$$F(\Delta) = 0 \quad \text{when } \Delta > D_{\max} \tag{5}$$

In this article, subscript A in Fig. 4 denotes the first loading direction and subscript B the opposite. The adopted sign convention is Δ, and F is positive on the A side and negative on the B side. The above equations are presented for the A side. For the B side, the sign of $F(\Delta)$ is changed and Δ is replaced by $|\Delta|$ in the equations. There are eight parameters to identify for monotonic loading: P_0, K_0, K_1, K_2, K_3, D_1, D_2, and $D_{\max}$.

One linear decreasing stiffness (K_2) and a cutting-off of strength may be sufficient to describe the monotonic curve of a nailed joint. Nevertheless, a more general model with second linear decreasing stiffness (K_3) was adopted to describe other types of connection in the same model. The value of K_2 is negative in most cases but could be positive when the relation is more ductile.

The cyclic loading rules are based on the four exponential hysteretic curves proposed by Dolan[9] to describe the pinching zone. These equations are modified by taking into account the load decrease by cyclic loading at the same displacement due to the damage to the wood and sliding.

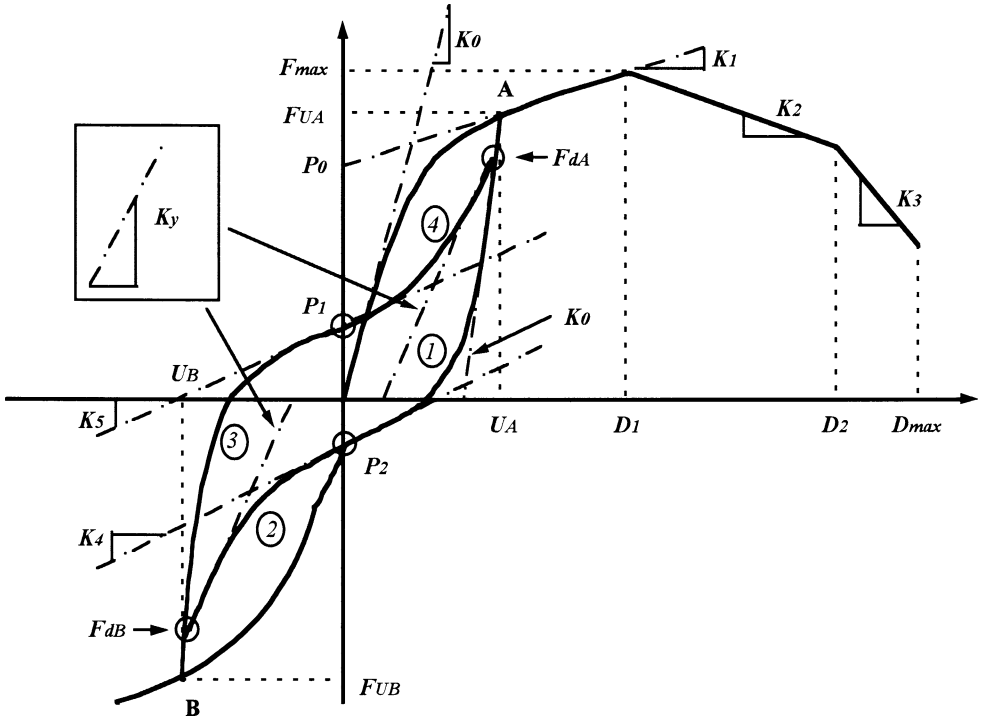

Fig. 4. Proposed load–slip model for the nailed connections

$$F(\Delta) = F_{dA} + (K_4\Delta + P_2 - F_{dA}) \times \left\{1 - \exp\left[K_0(U_A - \Delta)/(2P_2)\right]\right\} \quad \text{for part 1} \quad (6)$$

$$F(\Delta) = F_{dB} + (K_4\Delta + P_2 - F_{dB}) \times \left\{1 - \exp\left[-K_y(U_B - \Delta)/(2P_2)\right]\right\} \quad \text{for part 2} \quad (7)$$

$$F(\Delta) = F_{dB} + (K_5\Delta + P_1 - F_{dB}) \times \left\{1 - \exp\left[K_0(U_B - \Delta)/(2P_1)\right]\right\} \quad \text{for part 3} \quad (8)$$

$$F(\Delta) = F_{dA} + (K_5\Delta + P_1 - F_{dA}) \times \left\{1 - \exp\left[-K_y(U_A - \Delta)/(2P_1)\right]\right\} \quad \text{for part 4} \quad (9)$$

where K_4 is $\frac{P_2}{U_A}$, K_5 is $\frac{P_1}{U_B}$, and K_y is $\frac{F(D_y)}{D_y}$. D_y is the yield displacement determined from the experiment, and $F(D_y)$ is its corresponding force computed with the monotonic loading equation. U_A (or U_B) is the maximum (or minimum) slip reached during the previous loading history. Parts 1 to 4 represent the decreasing and reloading curves 1–4 in Fig. 4.

It is assumed that the decrease in strength by the second cycle loading in one direction (determining F_{dA} or F_{dB}) is proportional to the maximum load reached in the other direction F_{UB} (or F_{UA}) corresponding to U_B (or U_A):

$$F_{dA} = F_{UA} - \alpha_A\left[F_{UA} - (P_1 + K_5U_A)\right] \quad \text{with} \quad \alpha_A = k\left|\frac{F_{UB}}{F_{max}}\right| \quad (10)$$

$$F_{dB} = F_{UB} - \alpha_B\left[F_{UB} - (P_2 + K_4U_B)\right] \quad \text{with} \quad \alpha_B = k\left|\frac{F_{UA}}{F_{max}}\right| \quad (11)$$

The envelope curve is modified considering the decreased strength due to nail withdrawal. The postpeak monotonic strength ($|\Delta| > D_1$) is obtained by multiplying parameter β.

$$\beta_A = \gamma\left[\frac{U_A - D_1}{D_{max} - D_1}\right] \quad \text{and} \quad \beta_B = \gamma\left[\frac{U_B + D_1}{D_{max} - D_1}\right] \quad (12)$$

There are five more parameters to identify to complete the cyclic rules: P_1, P_2, D_y, k, and γ. All the parameters were determined from the reversed cyclic loading tests of the nailed joints.[10]

Model for beam-to-beam connections

Vertical and horizontal beams are connected by end nailing, a connection that is extremely weak. During the tests on the walls, we observed the progressive separation of vertical and horizontal beams at different locations of the structure in sole and sill plates and at the corner of the opening. Tension tests were conducted on such connections to obtain the load–slip relation. A bilinear brittle model in tension for pulling out of the nails and a higher stiffness in compression for unilateral contact are sufficient for approximating joint behavior. For cyclic loading, secant stiffness was adopted for unloading toward the origin and reloading on the same straight line. The peak load and two stiffness parameters are necessary to describe the load–slip curve. The load–slip relation of a nail joint in the lateral direction was not modeled, as the influence of a weaker link on the global behavior of the wall is not as important because the rotational strength of this kind of connection is so weak it was modeled with a perfect hinge.

Model for hold-down connections

On each side of the wall and at the bottom of an opening, hold-down connections were used to affix the structure to the foundation. These anchoring systems were placed at a distance from the bottom with four bolts. This connection was modeled with an element that links a fixed node located on the ground and the node of the corresponding vertical beam. The horizontal and rotary movements were free. The vertical slip obeys, in tension, a nonlinear law similar to the one used for the nail connection. In compression, high stiffness was taken to model the unilateral contact of the horizontal beam. The cyclic rules are simpler than those of the nail connection, as there is only one-way loading. P_1 and P_2 are equal to zero and so K_4 and K_5 remain null; and there is no strength degradation for cyclic loading at the same level. There are thus nine parameters for this connection model.

Results and discussion

Monotonic and cyclic tests

Figure 5 presents the comparison between the monotonic loading test results and simulation by the FE model. Although the initial stiffness was predicted accurately by the model, the maximum load tended to be overestimated. This may be caused by the variation in the sample, as only one wall was tested for monotonic loading.

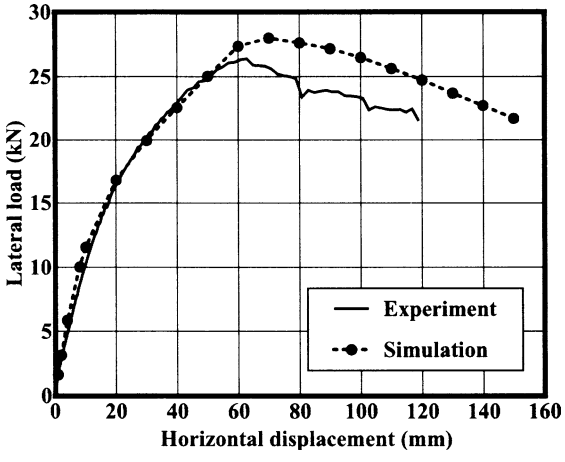

Fig. 5. Comparison of the simulation with experimental results for monotonic loading

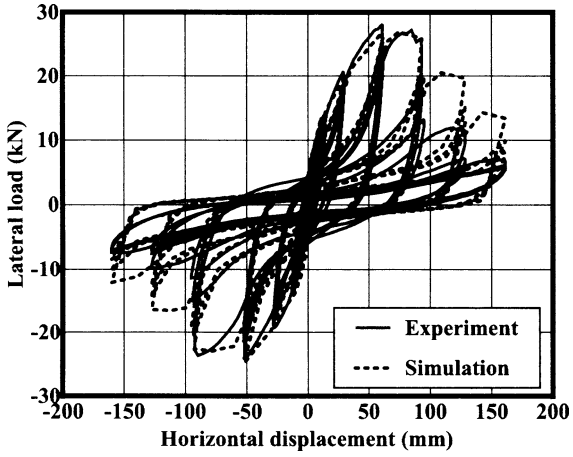

Fig. 6. Comparison of the simulation with experimental results for reversed cyclic loading

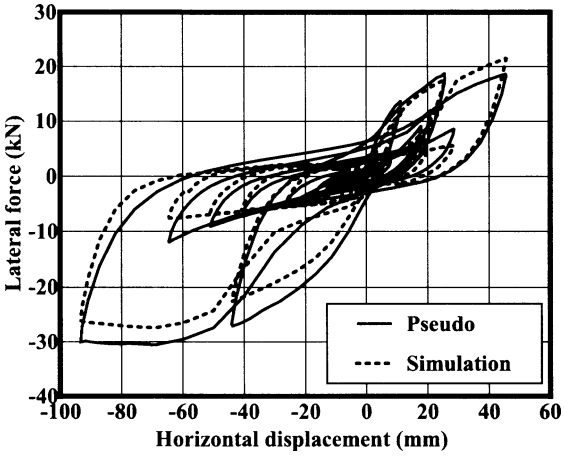

Fig. 8. Comparison of the simulation with experimental results in the pseudodynamic test with JMA Kobe earthquake records scaled to 0.4 g

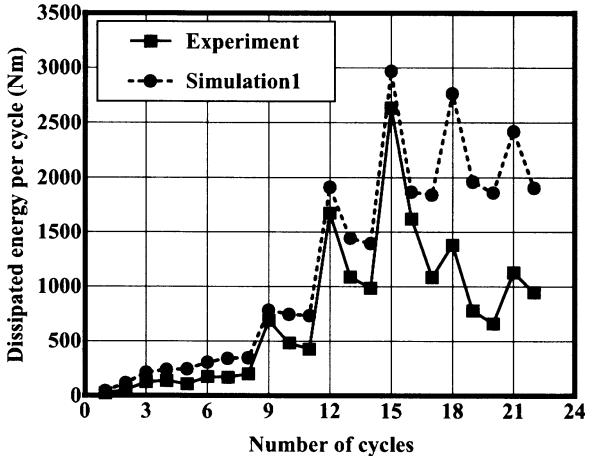

Fig. 7. Dissipated energy per cycle

The FE model is able to predict cyclic behavior of shear walls from the prescribed law for the hysteretic load path of nail joints. The simulated load–displacement relation from the imposed displacement is presented in Fig. 6, as are the results of reversed cyclic loading of the shear wall. The prediction by the FE model was correct for initial stiffness, maximum load, and the "pinching" zone. The decrease in the load between the first and second cycles was also accurately predicted. However, the model did not exactly fit the load–displacement relation after the peak load. It tended to overestimate the load on the first cycle and during cycles near the maximum displacement, but the "pinching zone" remained fairly well predicted. Differences between the experiment and the model at large displacement were more evident on the comparison of the dissipated energy per cycle (Fig. 7).

After the maximum load was attained, other damage was observed during the experiment. Adjacent panels were in contact and caused some major buckling of the side panels, especially on each side of the opening. This led to a rapid pull-through failure of a full row of nails near the opening. One way to model this phenomenon would be to use interpanel elements with a more complex, finite element to model the out-of-plane deflection. Another approach may be to apply different properties to nails.

Pseudodynamic tests

Two approaches are presented in this article for the pseudodynamic tests. The first is a static approach, equivalent to some set of cycles (described above). The second is a dynamic approach using the mass of the system and damping coefficients for the first and second modes of vibration.

The first approach obtains more information on the phenomenon law used for the connections. Figures 8 and 9 show a comparison between the force–displacement relations obtained from pseudodynamic tests and those calculated with the FE model using the input displacement of pseudodynamic test results with JMA Kobe and Landers earthquake accerelograms, respectively. For the Kobe earthquake, the shear force obtained from the simulation was slightly lower than the experimental results. Intermediate cycles were fairly calculated, but the simulation tended to underestimate the response. At around zero deflection, some weird values for the load given by the model tended to accentuate the "pinching" zone. This unrealistic calculus might come from the convergence trouble due to the fact that the signs of response and displacement were opposite. Small cycles around zero deflection are difficult to predict properly with this law used for connections.

For the Landers earthquake, different from the Kobe earthquake, the displacement increased continuously until maximum displacement was reached, then decreased slowly to almost zero displacement; the second large displacements occurred again before the final decrease. Each set of cycles was quite symmetrical. The initial stiffness and maximum load were well predicted by the simulation. Reloading cycles were fairly well modeled except for the cycling with extremely small displacement. In that case the predicted displacement response was again lower than the experimental results, as shown in Fig. 9a. Figure 9b shows the prediction that corresponds to the second set of accelerograms.

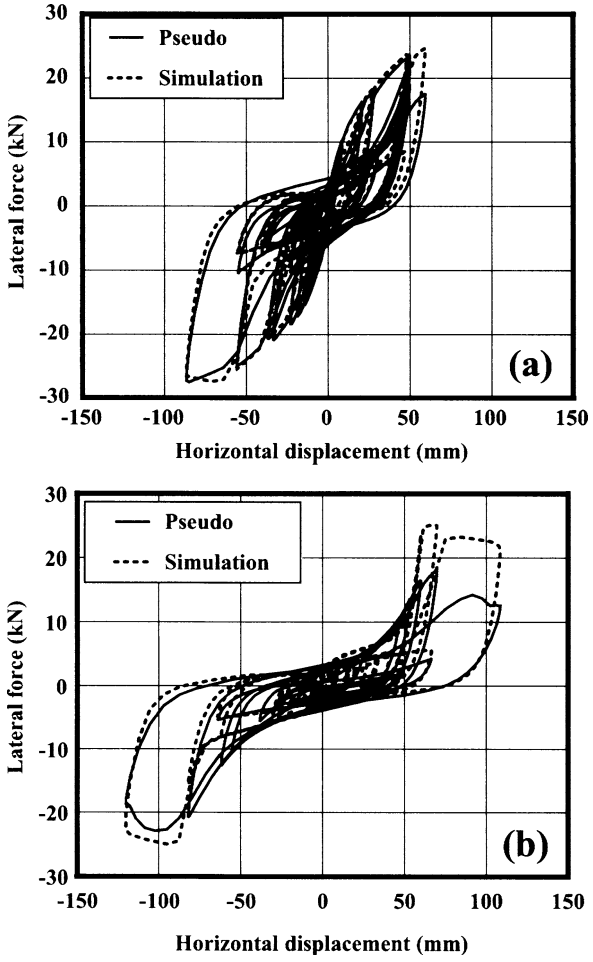

Fig. 9a,b. Comparison of the simulation with experimental results in the pseudodynamic test with Landers earthquake records scaled to 0.4 g. **a** First set of 18 s. **b** Second set of 18 s

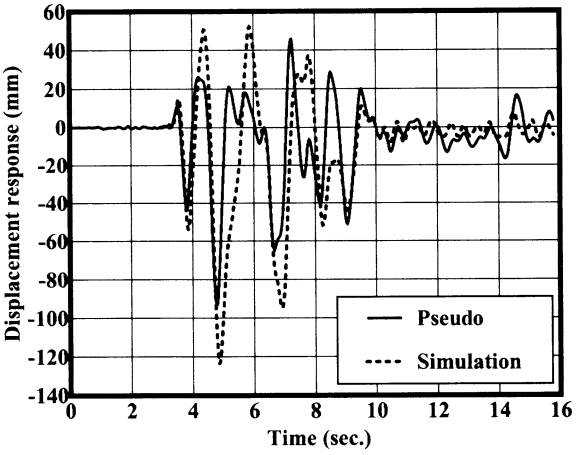

Fig. 10. Comparison of the simulated time-history displacement response with experimental results in the pseudodynamic test with JMA Kobe earthquake records scaled to 0.4 g

The large displacement in the negative direction was well predicted, but for the other direction the model tended to overestimate the response of the damaged specimen. Intermediate cycles were correctly predicted.

The second approach helps validate the curves obtained through dynamic simulation. Instead of imposing static displacement on the structure, the horizontal displacement was applied step by step by calculating the next step based on the lateral force response. During pseudodynamic tests, a computer calculated the new input displacement from the dynamic equations, including the mass on top of the structure, the damping coefficient applied to the first mode, and the response of the structure to the previously imposed displacement. The finite element code takes this information into account and does the same with the predicted response of the damaged structure derived from the nonlinear response of all the connections. Hence the variation in the calculated response directly influences the next displacement and so on.

Figures 10 and 11 compare the displacement response obtained from pseudodynamic tests and the dynamic analyses with JMA Kobe and Landers earthquake accelerograms, respectively. The period of the specimen was properly reproduced by the model, but the predicted response tended to show higher values than the experimental results for the Kobe earthquake. Note that this specimen had a high maximum load and stiffness, which influenced the response. For identical load levels, the model automatically predicted higher displacement than the experimental results. Moreover, the large calculated displacement tended to soften the response because of the sudden changes in displacement.

Figures 11a and 11b compare the time-history displacement response calculated by the FE model and the pseudodynamic test results with the first and the following 18 s of the Landers accelerograms, respectively. The first set of accelerograms showed quite good agreement with the experimental results. The second set was more difficult to predict properly owing to the previous damage to the specimen. The model was correct for most cycles but generally tended to overestimate the displacement response.

Conclusions

A finite element model for dynamic analysis of wood-framed shear walls is presented. The deterministic model assuming the independence of wood fiber orientation is sufficient for describing the behavior of a shear wall under monotonic, cyclic, and dynamic loading.[11,12] This numerical tool allows us to change the parameters easily, such as the configuration and location of nails, the connection of the walls to the foundation, the wall configuration, and so on. The hypothesis that the loading direction of nails remains constant during the simulation allows us to use unidirectional laws of the connection based on the experiment. Only one example of nail configuration was presented in this article, but any law can be now programmed in the code. Such a numerical tool could help us reduce the number of experiments. It can also be used to predict seismic behavior

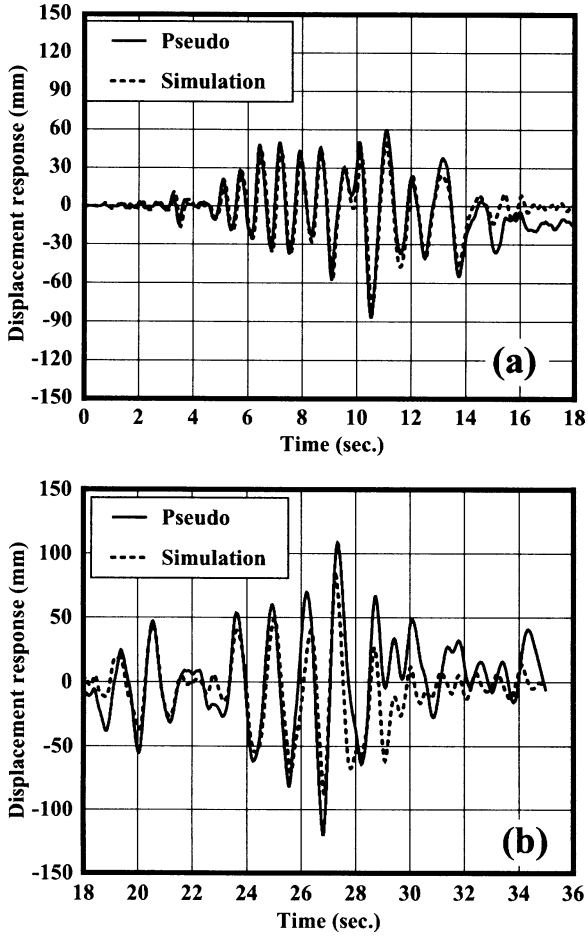

Fig. 11a,b. Comparison of the simulated time-history displacement response with experimental results in the pseudodyamic test with Landers earthquake records scaled to 0.4 g. **a** First set of 18 s **b** Second set of 18 s

of whole structures when we develop a macro model for three-dimensional structures.

References

1. Davenne L, Daudeville L, Kawai N, Yasumura M (1997) A numerical analysis of shear walls structural performances. In: Proceedings of the 30th CIB-W18, Vancouver, paper 30-15-3, pp 1–10
2. Davenne L, Daudeville L, Richard N, Kawai N, Yasumura M (1998) Modeling of timber shear walls with nailed joints under cyclic loading. In: Proceedings of the 1998 WCTE, vol 1, Montreux, pp 353–360
3. Daudeville L, Davenne L, Richard N, Kawai N, Yasumura M (1998) Numerical simulation of pseudo-dynamic tests performed to shear walls. In: Proceedings of the 31st CIB-W18, Savonlinna, paper 31-15-3, pp 1–12
4. Daudeville L, Davenne L, Richard N, Kawai N (1998) Etude du comportement parasismique de structures à ossature en bois. Rev Fr Genie Civil 2:651–665
5. Andreasson S, Yasumura M, Daudeville L (2002) Sensitivity study of FE-model for wood-framed shear walls. J Wood Sci 48:171–178
6. Ministry of Construction of Japan, notification 56, 1982
7. Richard N (2001) Approche multi-echelles pour la modelisation des structures en bois sous solicitations sismiques. Thèse de doctorat de l'Ecole Normale Supérieure de Cachan, LMT no. 2001/7
8. Foschi RO (1974) Load-slip characteristics of nails. Wood Sci 7(1):69–76
9. Dolan JD (1989) The dynamic response of timber shear walls. PhD thesis, University of British Columbia, Vancouver, BC
10. Yasumura M, Kawai N (1997) Evaluation of wood framed shear walls subjected to lateral load. In: Proceedings of the 30th CIB-W18, paper 30-15-4, pp 1–10
11. Filiatraut A (1990) Static and dynamic analysis of timber shear walls. Can J Civil Eng NRC 17:643–651
12. Tarabia AH, Kamiya F (1996) Analytical response of wood shear walls using hysteresis models of nailed joints (in Japanese). Mokuzai Gakkaishi 42:1064–1071